

4. A. M. Dondorp *et al.*, *N. Engl. J. Med.* **361**, 455 (2009).
5. H. Noedl *et al.*, *N. Engl. J. Med.* **359**, 2619 (2008).
6. N. J. White, *Science* **320**, 330 (2008).
7. P. Olliaro, T. N. Wells, *Clin. Pharmacol. Ther.* **85**, 584 (2009).
8. T. N. C. Wells, P. L. Alonso, W. E. Gutteridge, *Nat. Rev. Drug Discov.* **8**, 879 (2009).
9. E. A. Winzeler, *Nature* **455**, 751 (2008).
10. F. J. Gambo *et al.*, *Nature* **465**, 305 (2010).
11. W. A. Guiguemde *et al.*, *Nature* **465**, 311 (2010).
12. D. Plouffe *et al.*, *Proc. Natl. Acad. Sci. U.S.A.* **105**, 9059 (2008).
13. See supporting material on Science Online.
14. B. M. Russell *et al.*, *Antimicrob. Agents Chemother.* **47**, 170 (2003).
15. J. P. Guthmann *et al.*, *Trop. Med. Int. Health* **13**, 91 (2008).
16. N. J. White, *J. Antimicrob. Chemother.* **30**, 571 (1992).
17. W. W. Sharrock *et al.*, *Malar. J.* **7**, 94 (2008).
18. M. Traebert, B. Dumotier, *Expert Opin. Drug Saf.* **4**, 421 (2005).
19. N. J. White, *Lancet Infect. Dis.* **7**, 549 (2007).
20. B. N. Ames, F. D. Lee, W. E. Durston, *Proc. Natl. Acad. Sci. U.S.A.* **70**, 782 (1973).
21. D. A. Fidock, P. J. Rosenthal, S. L. Croft, R. Brun, S. Nwaka, *Nat. Rev. Drug Discov.* **3**, 509 (2004).
22. J. L. Vennerstrom *et al.*, *Nature* **430**, 900 (2004).
23. K. Hayton, X. Z. Su, *Curr. Genet.* **54**, 223 (2008).
24. A. Nzila, L. Mwai, *J. Antimicrob. Chemother.* **65**, 390 (2010).
25. P. K. Rathod, T. McErlean, P. C. Lee, *Proc. Natl. Acad. Sci. U.S.A.* **94**, 9389 (1997).
26. N. V. Dharia *et al.*, *Genome Biol.* **10**, R21 (2009).
27. M. J. Gardner *et al.*, *Nature* **419**, 498 (2002).
28. S. K. Volkman *et al.*, *Nat. Genet.* **39**, 113 (2007).
29. D. C. Jeffares *et al.*, *Nat. Genet.* **39**, 120 (2007).
30. L. J. Nkrumah *et al.*, *Nat. Methods* **3**, 615 (2006).
31. F. Trottein, J. Thompson, A. F. Cowman, *Gene* **158**, 133 (1995).
32. M. Dyer, M. Jackson, C. McWhinney, G. Zhao, R. Mikkelsen, *Mol. Biochem. Parasitol.* **78**, 1 (1996).
33. S. Krishna *et al.*, *J. Biol. Chem.* **276**, 10782 (2001).
34. L. Yatime *et al.*, *Biochim. Biophys. Acta* **1787**, 207 (2009).
35. W. Kühlbrandt, *Nat. Rev. Mol. Cell Biol.* **5**, 282 (2004).
36. A. M. Jensen, T. L. Sørensen, C. Olesen, J. V. Møller, P. Nissen, *EMBO J.* **25**, 2305 (2006).
37. D. M. Clarke, T. W. Loo, G. Inesi, D. H. MacLennan, *Nature* **339**, 476 (1989).
38. C. Toyoshima, M. Nakasako, H. Nomura, H. Ogawa, *Nature* **405**, 647 (2000).
39. C. Toyoshima, H. Nomura, *Nature* **418**, 605 (2002).
40. K. Moncoq, C. A. Trieber, H. S. Young, *J. Biol. Chem.* **282**, 9748 (2007).
41. M. Takahashi, Y. Kondou, C. Toyoshima, *Proc. Natl. Acad. Sci. U.S.A.* **104**, 5800 (2007).
42. M. C. Lee, P. A. Moura, E. A. Miller, D. A. Fidock, *Mol. Microbiol.* **68**, 1535 (2008).
43. P. Rice, I. Longden, A. Bleasby, *Trends Genet.* **16**, 276 (2000).
44. We thank A. Matter, M. Tanner, and P. Herrling for their foresight and support in establishing a malaria drug discovery program in the context of a public-private partnership. We thank T. A. Smith (SwissTPH) for the statistical analysis of the stage and rate of action studies. We thank S. Rao (Novartis Institute for Tropical Diseases) and M. Traebert (Novartis-preclinical safety), respectively, for the cytotoxicity and hERG inhibition data. We also thank M. Weaver (Novartis-preclinical safety) for the interpretation of the preclinical toxicology data. The team acknowledges P. Schultz, who had the vision to see the potential of the drug resistance experiments in the exploratory phase. In addition, we are grateful to R. T. Eastman for providing guidance to establish the in vitro drug-selection protocol and for providing the cloned Dd2 parasites. Finally, the scientific expertise provided by S. E. R. Bopp and S. K. Sharma and their helpful discussions throughout this project are greatly appreciated. Funding for the PfATP4 transfectants was provided to the Fidock laboratory in part by the Medicines for Malaria Venture (MMV08/0015; PI D. Fidock). The Shoklo Malaria Research Unit is sponsored by the Wellcome Trust of Great Britain, as part of the Oxford Tropical Medicine Research Programme of Wellcome Trust—Mahidol University. Laurent Renia's laboratory is supported by a core grant from the Singapore Immunology Network, A*STAR. This work was supported by a grant from the Medicines for Malaria Venture and a translational research grant (WT078285) from the Wellcome Trust to the Novartis Institute for Tropical Diseases, the Genomics Institute of the Novartis Research Foundation and the Swiss Tropical Institute, and by grants to E.A.W. from the W. M. Keck Foundation and the NIH (R01AI059472). NITD609 is described in the Novartis patent application WO2009/132921. All requests for spiroindolones or related compounds are subject to a Material Transfer Agreement. T.H.K. and E.A.W. own shares in Novartis (Switzerland).

Supporting Online Material

www.sciencemag.org/cgi/content/full/329/5996/1175/DC1
Materials and Methods
Figs. S1 to S10
Tables S1 to S13
References

3 June 2010; accepted 20 June 2010
10.1126/science.1193225

REPORTS

Detection of C₆₀ and C₇₀ in a Young Planetary Nebula

Jan Cami,^{1,2*} Jeronimo Bernard-Salas,^{3,4} Els Peeters,^{1,2} Sarah Elizabeth Malek¹

In recent decades, a number of molecules and diverse dust features have been identified by astronomical observations in various environments. Most of the dust that determines the physical and chemical characteristics of the interstellar medium is formed in the outflows of asymptotic giant branch stars and is further processed when these objects become planetary nebulae. We studied the environment of Tc 1, a peculiar planetary nebula whose infrared spectrum shows emission from cold and neutral C₆₀ and C₇₀. The two molecules amount to a few percent of the available cosmic carbon in this region. This finding indicates that if the conditions are right, fullerenes can and do form efficiently in space.

Interstellar dust makes up only a small fraction of the matter in our galaxy, but it plays a crucial role in the physics and chemistry of the interstellar medium (ISM) and star-forming regions (1). The bulk of this dust is created in the outflows of old, low-mass asymptotic giant branch (AGB) stars; such outflows are slow (5 to 20 km/s) but massive (10⁻⁸ to 10⁻⁴ solar masses per year)

(2–4). Once most of the envelope is ejected, the AGB phase ends and the stellar core—a hot white dwarf—becomes gradually more exposed. When this white dwarf ionizes the stellar ejecta, they become visible as a planetary nebula (PN).

Chemical reactions and nucleation in the AGB outflows transform the atomic gas into molecules and dust grains. For carbon-rich AGB stars (sometimes called carbon stars), this results in a large variety of carbonaceous compounds; to date, more than 60 individual molecular species and a handful of dust minerals have been identified in these outflows (5), including benzene, polyynes, and cyanopolyynes up to about 13 atoms in size (6, 7).

These environments are also thought to be the birthplace for large aromatic species such as

polycyclic aromatic hydrocarbons (PAHs) and fullerenes (8, 9), a class of large carbonaceous molecules that were discovered in laboratory experiments aimed at understanding the chemistry in carbon stars (10). Fullerenes have unique physical and chemical properties, and the detection of fullerenes and the identification of their formation site are therefore considered a priority in the field of interstellar organic chemistry (11). However, astronomical searches for fullerenes in interstellar and circumstellar media have not resulted in conclusive evidence (12–14). The most promising case to date is the detection of two diffuse interstellar bands (DIBs) in the near-infrared (15) whose wavelengths are close to laboratory spectra of C₆₀⁺ in solid matrices (16); this finding awaits confirmation from comparison to a cold, gas-phase spectrum.

Here, we report on the detection of the fullerenes C₆₀ and C₇₀ in the circumstellar environment of Tc 1. Tc 1 is a young, low-excitation PN where the white dwarf is still enshrouded by the dense stellar ejecta. At optical wavelengths, Tc 1 shows H α emission up to ~50 arc sec away from the central star, but the PN also has a much smaller (~9 arc sec) and more compact core that was observed with the Infrared Spectrograph (IRS) (17) onboard the Spitzer Space Telescope (18). This inner region turns out to be carbon-rich, hydrogen-poor, and dusty.

The Spitzer IRS spectrum of Tc 1 (Fig. 1) (19) shows numerous narrow forbidden emission

¹Department of Physics and Astronomy, University of Western Ontario, London, Ontario N6A 3K7, Canada. ²SETI Institute, 515 North Whisman Road, Mountain View, CA 94043, USA. ³222 Space Sciences Building, Cornell University, Ithaca, NY 14853, USA. ⁴Institut d'Astrophysique Spatiale, CNRS/Université Paris-Sud 11, 91405 Orsay, France.

*To whom correspondence should be addressed. E-mail: jcam@uwo.ca

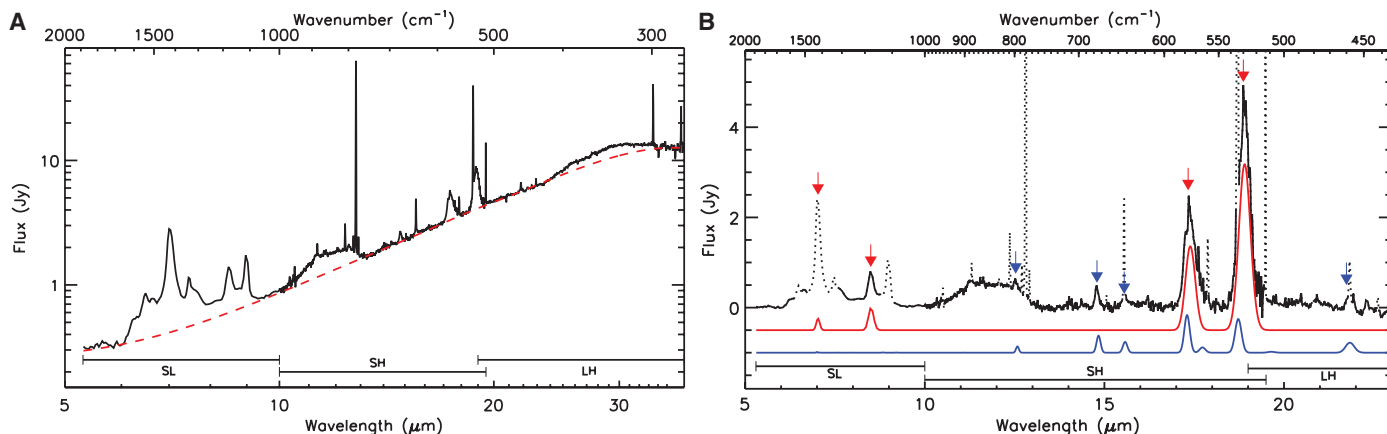


Fig. 1. The Spitzer IRS spectrum of Tc 1. **(A)** The entire range, 5 to 37 μm . **(B)** Continuum-subtracted spectrum between 5 and 23 μm , where known forbidden emission lines are masked (19). We fitted a cubic spline to spectral ranges devoid of features to determine the dust continuum (red dashed line). The broad plateau between 11 and 13 μm is attributed to emission from SiC dust (34, 35), and the well-known broad feature longward of 23 μm is believed to be due to MgS (36). Red arrows mark the wavelengths of all infrared active modes for C_{60} ; blue arrows denote those of the four strongest, isolated

C_{70} bands. The red and blue curves below the data are thermal emission models for all infrared active bands of C_{60} and C_{70} at temperatures of 330 K and 180 K, respectively (19). We convolved the bands with a Gaussian profile ($\sigma = 2.55 \text{ cm}^{-1}$ for all C_{70} bands, $\sigma = 4.5 \text{ cm}^{-1}$ for the C_{60} bands in the SH/LH module, and $\sigma = 10 \text{ cm}^{-1}$ for those in the SL module). Apparent weak emission bumps near 14.4, 16.2, 20.5, and 20.9 μm are artifacts. The nature of the weak feature near 22.3 μm is unclear because it appears differently in both nods.

lines that are characteristic for the low-density gas environment of PNe. The infrared continuum is due to emission from circumstellar dust. For carbon-rich environments, this dust is typically amorphous carbon, which results in a featureless continuum. Other common dust components reveal their presence through emission bands.

The spectra of most carbon-rich PNe are generally dominated by strong emission features due to PAHs. These features are completely absent in the spectrum of Tc 1. In addition, there is no trace of even the simplest H-containing molecules (such as HCN and C_2H_2) that are often observed in carbon-rich proto-PNe. The Spitzer IRS spectrum does show a few weak hydrogen recombination lines, but these most likely originate from the halo material farther out, where $\text{H}\alpha$ emission is also observed. Instead, the spectrum is dominated by the prominent C_{60} bands at 7.0 (20), 8.5, 17.4, and 18.9 μm , and furthermore exhibits weaker features that are due to C_{70} (Fig. 1).

Emission processes result in band intensities that are proportional to the Einstein A coefficients for spontaneous emission and to the population of the excited states. We scaled the experimentally obtained relative absorption coefficients for the C_{60} bands (1, 0.48, 0.45, and 0.378 for the bands at 18.9, 17.4, 8.5, and 7.0 μm , respectively) (21, 22) to absolute values by adopting a value of 25 km/mol for the band at 8.5 μm (23) and converted them to Einstein A coefficients. Using these, we calculated the population distribution over the excited vibrational states from the total emitted power in each of the C_{60} bands and found them to be consistent with thermal emission, in which case they are fully determined by a single parameter—the excitation temperature—which we derived to be $\sim 330 \text{ K}$ (19). The relative intensities of the infrared C_{60} bands in Tc 1 thus match what is ex-

pected for thermal emission at 330 K when using experimentally obtained absorption coefficients.

It is well established from laboratory experiments that the peak wavelengths and bandwidths are temperature-dependent (24). The peak wavelengths in Tc 1 agree, within uncertainty, with those found in laboratory experiments obtained at temperatures comparable to our derived excitation temperature (19, 25). We measured widths (full width at half maximum) of $\sim 10 \text{ cm}^{-1}$ for the bands at 18.9 and 17.4 μm , which agrees with laboratory results (24–26); the bands at 7.0 and 8.5 μm are unresolved (19). We performed a similar analysis for the C_{70} bands using appropriate laboratory results (24, 27, 28) and obtained an excitation temperature of $\sim 180 \text{ K}$ (19).

For comparison, we used the derived excitation temperatures to construct thermal emission models for both molecules (Fig. 1). The correspondence between the laboratory-based emission model and the observations supports the identification of these bands with fullerenes. The absence of the corresponding spectral features of fullerene cations or anions (e.g., 7.1 and 7.5 μm for C_{60}^+) implies that the fullerenes are in the neutral state. All infrared active bands of both species are fully accounted for in Tc 1; no other clear spectral features remain unidentified in the spectrum (19). The environment of Tc 1 thus results in a unique dust composition, but not in a wide variety of dust components.

Our results suggest that the emission does not originate from free molecules in the gas phase, but from molecular carriers attached to solid material. With an effective temperature for the central object of $\sim 30,000 \text{ K}$, the radiation field peaks for photon energies in the range 6 to 10 eV, which would result in excitation temperatures of 800 to 1000 K for large gas-phase species. The much

lower temperatures derived for the fullerenes thus imply that these species are in direct contact with a much cooler material. In this environment, the most likely solid material is the surface of the abundant carbonaceous grains present in the outflow. These solids are in radiative equilibrium with the stellar radiation field, and thus their temperature is determined by the distance from the central object. If the fullerenes are in direct contact with this material, they must be at the same temperature and display a thermal population distribution over the excited vibrational states, such as we observe in Tc 1. The difference in temperature between C_{60} and C_{70} then implies different spatial locations, with C_{60} located closer to the illuminating source than C_{70} . This could happen if C_{70} forms from C_{60} as it moves out.

The presence of only neutral fullerenes is in agreement with an origin on grain surfaces, in which case charge effects on individual molecules are unimportant. In contrast, gaseous C_{60} would be largely in cationic form in this environment. Some observational support for an origin in the solid state is also provided by the broad and generally symmetric (Gaussian) band profiles. For gas-phase species, vibrational anharmonicities (and possibly ro-vibrational structure) would result in asymmetric bands. Only a small fraction of such gaseous material could be hidden in the observed bands. The absence of gas-phase species is puzzling and could indicate that the fullerenes form on (or from) the dust grains and never fully evaporate.

On Earth, fullerenes can be synthesized by vaporizing graphite in a hydrogen-poor atmosphere that contains helium as a buffer gas. The fullerene formation process is very efficient, and C_{60} is by far the dominant and most stable species among the large cluster population formed in

these experiments, followed by C_{70} (10, 25). However, fullerene formation is inhibited by the presence of hydrogen (29, 30). The circumstellar environment of Tc 1 seems to be the astrophysical analog of such a laboratory setup. The dust is clearly carbonaceous—as is also expected from the overabundance of C in the gas phase, with a C/O ratio of ~ 3.2 (31)—but the absence of any H-containing species indicates that the dust environment must be very H-poor. About 5.8×10^{-8} solar masses of pure C_{60} and $\sim 4.7 \times 10^{-8}$ solar masses of C_{70} are required to reproduce the emission bands. The Spitzer IRS observations are sensitive to dust only at temperatures of at least ~ 100 K, and given the measured expansion velocity of 20 km/s (32), this corresponds to mass loss from only the past 100 years. At the measured carbon abundance (31) and adopting a mass loss rate of 10^{-4} solar masses per year, this means that each of the fullerene species represents at least $\sim 1.5\%$ of the available carbon. This is roughly consistent with abundance estimates from the two DIBs associated with C_{60}^+ (15) and matches the fraction of graphite that is converted into fullerenes in laboratory experiments (25). Fullerenes can also be created by photochemical processing of hydrogenated amorphous carbon (33). However, such processes generally also result in large amounts of PAHs, which are absent in Tc 1. The role of photochemistry in the fullerene formation process in Tc 1 is thus unclear.

The unusual circumstellar environment of Tc 1 indicates that it must have ejected its entire hydrogen envelope at least a few thousand years ago, exposing the helium intershell material. Presumably, a late thermal pulse then caused the ejection of this material, which now makes up the warm, dusty, and hydrogen-poor PN core where fullerenes are abundant. Tc 1 is thus not neces-

sarily an unusual object, although we evidently have observed it during a short (and possibly unusual) phase. The presence or absence of hydrogen in this type of carbon-rich environment then clearly determines whether the chemical pathways favor the formation of PAH molecules or fullerenes as large aromatic species. Within the context of carbon-rich PNe, the PAH route is generally dominant; only those objects that completely remove their hydrogen envelope and undergo a late thermal pulse can then create the hydrogen-poor environment where fullerenes flourish.

References and Notes

- A. G. G. M. Tielens, *The Physics and Chemistry of the Interstellar Medium* (Cambridge Univ. Press, Cambridge, 2005).
- H. J. Habing, *Astron. Astrophys. Rev.* **7**, 97 (1996).
- L. A. Willson, *Annu. Rev. Astron. Astrophys.* **38**, 573 (2000).
- F. Herwig, *Annu. Rev. Astron. Astrophys.* **43**, 435 (2005).
- S. Kwok, *Int. J. Astrobiol.* **8**, 161 (2009).
- J. Cernicharo *et al.*, *Astrophys. J.* **546**, L123 (2001).
- J. R. Pardo, J. Cernicharo, J. R. Goicoechea, M. Guélin, A. Asensio Ramos, *Astrophys. J.* **661**, 250 (2007).
- M. Frenklach, E. D. Feigelson, *Astrophys. J.* **341**, 372 (1989).
- I. Cherchneff, Y. H. Le Teuff, P. M. Williams, A. G. G. M. Tielens, *Astron. Astrophys.* **357**, 572 (2000).
- H. W. Kroto, J. R. Heath, S. C. O'Brien, R. F. Curl, R. E. Smalley, *Nature* **318**, 162 (1985).
- E. Herbst, E. F. van Dishoeck, *Annu. Rev. Astron. Astrophys.* **47**, 427 (2009).
- G. H. Herbig, *Astrophys. J.* **542**, 334 (2000).
- C. Moutou, K. Sellgren, L. Verstraete, A. Léger, *Astron. Astrophys.* **347**, 949 (1999).
- G. C. Clayton *et al.*, *Astron. J.* **109**, 2096 (1995).
- B. H. Foing, P. Ehrenfreund, *Nature* **369**, 296 (1994).
- J. Fulara, M. Jakobi, J. P. Maier, *Chem. Phys. Lett.* **211**, 227 (1993).
- J. R. Houck *et al.*, *Astrophys. J.* **154** (suppl.), 18 (2004).
- M. W. Werner *et al.*, *Astrophys. J.* **154** (suppl.), 1 (2004).
- See supporting material on Science Online.
- The emission at $7.0 \mu\text{m}$ is much higher than expected for C_{60} emission alone because of a blend with a strong [ArII] line.
- M. C. Martin, D. Koller, L. Mihaly, *Phys. Rev. B* **47**, 14607 (1993).
- J. Fabian, *Phys. Rev. B* **53**, 13864 (1996).
- N. Sogoshi *et al.*, *J. Phys. Chem. A* **104**, 3733 (2000).
- L. Nemes *et al.*, *Chem. Phys. Lett.* **218**, 295 (1994).
- W. Krättschmer, L. D. Lamb, K. Fostiropoulos, D. R. Huffman, *Nature* **347**, 354 (1990).
- C. I. Frum *et al.*, *Chem. Phys. Lett.* **176**, 504 (1991).
- A. von Czarowski, K. H. Meiwes-Broer, *Chem. Phys. Lett.* **246**, 321 (1995).
- R. Stratmann, G. Scuseria, M. Frisch, *J. Raman Spectrosc.* **29**, 483 (1998).
- M. S. De Vries *et al.*, *Geochim. Cosmochim. Acta* **57**, 933 (1993).
- X. K. Wang *et al.*, *J. Mater. Res.* **10**, 1977 (1995).
- Y. V. Milanova, A. F. Kholytygin, *Astron. Lett.* **35**, 518 (2009).
- A. Acker, K. Gesicki, Y. Grosdidier, S. Durand, *Astron. Astrophys.* **384**, 620 (2002).
- A. Scott, W. W. Duley, G. P. Pinho, *Astrophys. J.* **489**, L193 (1997).
- A. K. Speck, A. B. Corman, K. Wakeman, C. H. Wheeler, G. Thompson, *Astrophys. J.* **691**, L202 (2009).
- J. Bernard-Salas *et al.*, *Astrophys. J.* **699**, 1541 (2009).
- S. Hony, L. B. F. M. Waters, A. G. G. M. Tielens, *Astron. Astrophys.* **390**, 533 (2002).
- We thank M. Houde and A. Tielens for commenting on earlier versions of the manuscript, G. Fanchini for stimulating discussions on various properties of fullerene materials, and G. C. Sloan for discussions on carbonaceous species in PNe. Supported by a Discovery grant from the National Science and Engineering Research Council of Canada (J.C., E.P., and S.E.M.) and by the Spitzer Space Telescope General Observer Program.

Supporting Online Material

www.sciencemag.org/cgi/content/full/science.1192035/DC1
Materials and Methods
Fig. S1
Table S1
References

10 May 2010; accepted 7 July 2010

Published online 22 July 2010;

10.1126/science.1192035

Include this information when citing this paper.

Real-Time Dynamics of Single Vortex Lines and Vortex Dipoles in a Bose-Einstein Condensate

D. V. Freilich,* D. M. Bianchi,† A. M. Kaufman,‡ T. K. Langin, D. S. Halls

Understanding the behavior of quantized vortices is essential to gaining insight into diverse superfluid phenomena, from critical-current densities in superconductors to quantum turbulence in superfluids. We observe the real-time dynamics of quantized vortices in trapped dilute-gas Bose-Einstein condensates by repeatedly imaging the vortex cores. The precession frequency of a single vortex is measured by explicitly observing its time dependence and is found to be in good agreement with theory. We further characterize the dynamics of vortex dipoles in two distinct configurations: (i) an asymmetric configuration, in which the vortex trajectories are dynamic and nontrivial, and (ii) a stable, symmetric configuration, in which the dipole is stationary.

Quantized vortices are topological defects that carry angular momentum and are among the most conspicuous characteristics of a superfluid (1, 2). Although superfluid phenomena have been recognized for more than

a century, it is only in the past few decades that the motion of quantized vortex lines has been detected in real time through magnetic resonance techniques, including the precession of a single vortex line (3), the propagation of vortices from a

rotating superfluid into a nonrotating superfluid (4, 5), and the phase transition of vortex lines into vortex sheets (6). The dynamical behavior of quantized vortex lines has also been imaged directly in real time in superfluid helium (7) and type II superconductors (8). These studies have yielded a wealth of information about how vortices influence superfluid behavior through their pinning, transport, and reconnection properties.

Dilute-gas Bose-Einstein condensates (BECs) (9–11) are a natural choice for fundamental studies

Department of Physics, Amherst College, Amherst, MA 01002–5000, USA.

*Present address: Department of Mechanical and Aerospace Engineering, University of California, San Diego, La Jolla, CA 92093–0411 USA.

†Present address: Department of Linguistics and Philosophy, Massachusetts Institute of Technology, Cambridge, MA 02139–4307 USA.

‡Present address: JILA, National Institute of Standards and Technology and Department of Physics, University of Colorado, Boulder, CO 80309–0440, USA.

§To whom correspondence should be addressed. E-mail: dshall@amherst.edu

This copy is for your personal, non-commercial use only.

If you wish to distribute this article to others, you can order high-quality copies for your colleagues, clients, or customers by [clicking here](#).

Permission to republish or repurpose articles or portions of articles can be obtained by following the guidelines [here](#).

The following resources related to this article are available online at www.sciencemag.org (this information is current as of September 13, 2010):

Updated information and services, including high-resolution figures, can be found in the online version of this article at:

<http://www.sciencemag.org/cgi/content/full/329/5996/1180>

Supporting Online Material can be found at:

<http://www.sciencemag.org/cgi/content/full/science.1192035/DC1>

A list of selected additional articles on the Science Web sites **related to this article** can be found at:

<http://www.sciencemag.org/cgi/content/full/329/5996/1180#related-content>

This article has been **cited by** 1 articles hosted by HighWire Press; see:

<http://www.sciencemag.org/cgi/content/full/329/5996/1180#otherarticles>

This article appears in the following **subject collections**:

Astronomy

<http://www.sciencemag.org/cgi/collection/astronomy>